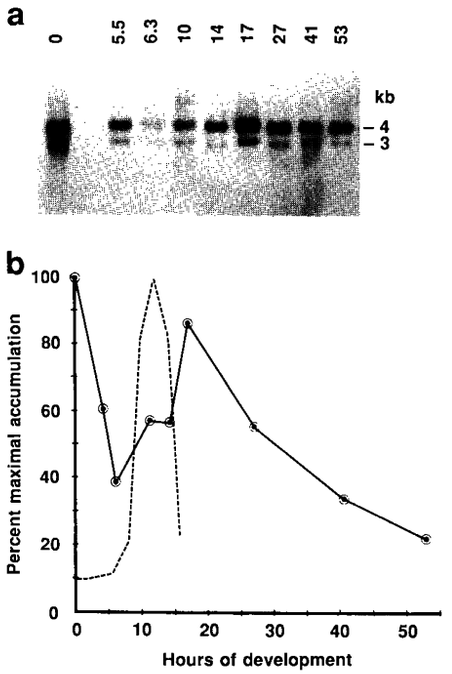

Fig. 5. Time course of uEGF transcript accumulation. (**a**) RNA gel blot analysis, carried out as described in Fig. 1. Numbers above the lanes indicate hours of development at 13°C. These times represent the following developmental stages; 0 hours, unfertilized egg; 5.5 hours, 8-cell stage; 6.3 hours, 16-cell stage; 10 hours, late-cleavage stage; 14 hours, prehatching blastula; 17 hours, late-hatched blastula; 27 hours, mesenchyme blastula; 41 hours, early gastrula; 53 hours, late gastrula. (**b**) Quantification by densitometry of RNA gel blot data. The ordinate represents hours of development at 13°C. The abscissa represents arbitrary values relative to the maximal accumulation level. (●) The behavior of the uEGF transcript; the results shown are the average of two blots, one of which is shown in (a). The dashed line represents the accumulation of the α histones and was plotted from (*36*).

synthesis of histones in this embryo correlates with the rate of cell division (*24*). Because the second period of uEGF message accumulation occurs after the rapid cell divisions of early cleavage, we do not expect uEGF to be operating solely as a stimulator of cell proliferation in this system. The transcripts of many lineage-specific genes in sea urchins first appear at the blastula stage; they accumulate asynchronously, but their midpoints of accumulation all occur after the midpoint of accumulation of the uEGF transcript (*25–27*).

Some mammalian members of the EGF family are thought to act as regulators of cell proliferation and differentiation (*1, 28*). The EGF-like molecules encoded by *notch* and *lin 12* are involved in the specification of embryonic cell fates (*29, 30*). The behavior of the uEGF transcript, whose accumulation precedes known molecular indices of cell differentiation, as well as the structural similarity of the uEGF gene to other invertebrate binary switch genes, suggests that it too may play an important role in embryogenesis. Whatever its function, the existence of this highly conserved sequence in the echinoderms indicates that the EGF peptide domain predates the radiation of coelomate animals and has been retained in a number of diverse evolutionary lineages.

REFERENCES AND NOTES

1. G. Carpenter and S. Cohen, *Annu. Rev. Biochem.* **48**, 193 (1979).
2. K. A. Wharton, K. M. Johansen, T. Xu, S. Artavanis-Tsakonas, *Cell* **43**, 567 (1985).
3. S. Kidd, M. R. Kelley, M. W. Young, *Mol. Cell Biol.* **6**, 3094 (1986).
4. I. Greenwald, *Cell* **43**, 583 (1985).
5. M. A. Harkey and A. H. Whiteley, *Wilhelm Roux Arch. Dev. Biol.* **189**, 111 (1980).
6. D. McClay and A. F. Chambers, *Dev. Biol.* **63**, 179 (1978).
7. T. Maruyama, T. Gojobori, S.-I. Aota, T. Ikemura, *Nucleic Acids Res.* **14** (suppl.) r151 (1986).
8. D. J. Lipman and W. R. Pearson, *Science* **227**, 1435 (1985).
9. R. F. Doolittle, D. F. Feng, M. S. Johnson, *Nature (London)* **307**, 558 (1984).
10. J. P. Brown, D. R. Twardzik, H. Marquardt, G. J. Todaro, *ibid.* **313**, 491 (1985).
11. H. Marquardt, M. W. Hunkapiller, L. E. Hood, G. J. Todaro, *Science* **223**, 1079 (1984).
12. D. Pennica *et al.*, *Nature (London)* **301**, 214 (1983).
13. B. A. McMullen *et al.*, *Biochemistry* **22**, 2875 (1983).
14. D. L. Enfield *et al.*, *ibid.* **19**, 659 (1980).
15. D. W. Russell *et al.*, *Cell* **37**, 577 (1985).
16. R. W. Jackman *et al.*, *Proc. Natl. Acad. Sci. U.S.A.* **83**, 8834 (1986).
17. J. Hoskins, D. K. Norman, R. J. Beckman, G. L. Long, *ibid.* **84**, 349 (1987).
18. J. Stenflo, A. Lundwall, B. Dahlback, *ibid.*, p. 368.
19. T. Nikaido *et al.*, *Nature (London)* **311**, 631 (1985).
20. J. Kyte and R. F. Doolittle, *J. Mol. Biol.* **157**, 105 (1982).
21. R. C. Angerer and E. H. Davidson, *Science* **226**, 1153 (1984).
22. C. N. Flytzanis, B. P. Brandhorst, R. J. Britten, E. H. Davidson, *Dev. Biol.* **91**, 27 (1982).
23. E. H. Davidson, *Gene Activity in Early Development* (Academic Press, New York, 1976).
24. B. Moav and M. Nemer, *Biochemistry* **10**, 881 (1971).
25. W. H. Klein *et al.*, in *Time, Space, and Pattern in Embryonic Development*, W. R. Jeffery and R. A. Raff, Eds. (Liss, New York, 1983), pp. 87–100.
26. R. J. Shott *et al.*, *Dev. Biol.* **101**, 295 (1984).
27. D. S. Leaf *et al.*, *ibid.* **121**, 29 (1987).
28. D. R. Twardzik, J. E. Ranchalis, G. J. Todaro, *Cancer Res.* **42**, 590 (1982).
29. I. S. Greenwald, P. W. Sternberg, H. R. Horvitz, *Cell* **34**, 435 (1983).
30. B. Yedvobnik *et al.*, *Cold Spring Harbor Symp. Quant. Biol.* **50**, 841 (1985).
31. D. A. Hursh and R. A. Raff, in preparation.
32. J. Messing, *Methods Enzymol.* **101**, 20 (1983).
33. F. Sanger, S. Nicklen, A. R. Coulson, *Proc. Natl. Acad. Sci. U.S.A.* **74**, 5463 (1977).
34. A. J. H. Smith, *Methods Enzymol.* **65**, 560 (1980).
35. M. D. Biggin, T. J. Gibson, G. F. Hong, *Proc. Natl. Acad. Sci. U.S.A.* **80**, 3963 (1983).
36. D. E. Wells *et al.*, *Wilhelm Roux Arch. Dev. Biol.* **195**, 252 (1986).

37. We thank T. Thomas for providing the cDNA libraries used in this study. We thank E. Raff, B. Parr, D. Leaf, P. Cherbas, and M. Muskavitch for critical comments regarding the manuscript. Supported by NIH grant R01 HD21986. D.A.H. was supported by an NIH predoctoral training grant.

23 March 1987; accepted 26 June 1987

Acantharian Fluxes and Strontium to Chlorinity Ratios in the North Pacific Ocean

R. E. BERNSTEIN, P. R. BETZER, R. A. FEELY, R. H. BYRNE, M. F. LAMB, A. F. MICHAELS

Data on particulate strontium sulfate fluxes and strontium to chlorinity ratios were compared to provide insights into the strontium cycle of the North Pacific. Free-drifting sediment traps were used to derive large particle fluxes between depths of 100 and 3500 meters in the eastern and western North Pacific Ocean. Flux data revealed substantial quantities of acantharian skeletons and cysts (both made of strontium sulfate) settling through the upper kilometer of the water column. The greatest fluxes of celestite were detected at 400 meters. Minimal to nondetectable fluxes noted at and below 900 meters provide evidence that by this horizon, the majority of acantharian specimens had dissolved, thereby contributing to the pool of dissolved strontium. Growth and subsequent dissolution of acantharians in the upper kilometer are qualitatively consistent with the well-developed minimum and maximum strontium to chlorinity ratios that are consistently noted in these waters. These fluxes of particulate strontium and model calculations for fluxes of dissolved strontium indicate that acantharians play an important role in the ocean's strontium budget.

THE GLOBAL OCEANIC STRONTIUM budget may be dramatically affected by the only marine organisms to use Sr as a major skeletal component. These abundant organisms, the acantharians, are marine planktonic protists that secrete a

R. E. Bernstein, P. R. Betzer, R. H. Byrne, Department of Marine Science, University of South Florida, St. Petersburg, FL 33701.
R. A. Feely and M. F. Lamb, Pacific Marine Environmental Laboratory, National Oceanic and Atmospheric Administration, Seattle, WA 98115.
A. F. Michaels, Institute of Marine Sciences, University of California, Santa Cruz, CA 95060.

skeleton made of celestite ($SrSO_4$). An encystment stage associated with reproduction has been described for some acantharians (*1–3*); the cyst also consists of $SrSO_4$.

Study of acantharian ecology, which had waned after the turn of the century, has seen a resurgence within the last two decades. The hiatus may be the result of problems associated with acantharian preservation in samples, as well as a lack of acantharian representation in marine sediments (*4, 5*). Both situations are caused by rapid dissolution of acantharian specimens. Subsequent interest in acantharians might be attributed to new and diverse sampling and preservation techniques that show acantharians to be highly abundant zooplankters (*6–11*). Because of their abundance, acantharians are implicated as an important component in geochemical Sr cycling (*12*) and are potentially important as carriers of ^{90}Sr (*9*) and trace metals (*9, 13, 14, 15*).

Since the first quantitative data on dissolved Sr were reported by Desgrez and Meunier in 1926 (*16*), dissolved Sr has been analyzed by a variety of procedures with diverse results (*12, 17–21*). Early work in the Atlantic, Pacific, and Arctic oceans by Chow and Thompson (*18*) indicated that dissolved Sr was a conservative element with a Sr/Cl ratio near 416 μg/g. More recent work, in which refined measuring techniques were used, has provided evidence of variable Sr/Cl ratios with depth (*12, 20, 21*). Brass and Turekian (*21*) showed a Sr/Cl profile for the North Pacific where the Sr/Cl ratio varied from 396 to 405, indicating a depletion of dissolved Sr in the surface waters. In keeping with the suggestion of Brass and Turekian (*12*), it is our contention that variations in Sr/Cl ratios are the result of both growth and dissolution of acantharian skeletons and cysts. All ocean waters are highly undersaturated with respect to $SrSO_4$, and acantharian specimens have been reported to dissolve rapidly within the water column after the organism's death (*4, 8*). The implication that acantharian growth and subsequent dissolution affect the oceanic Sr budget is reinforced by studies carried out in the Atlantic, the Pacific, the Mediterranean, and in several coastal zones of the Ligurian, Tyrrhenian, Ionian, and Adriatic

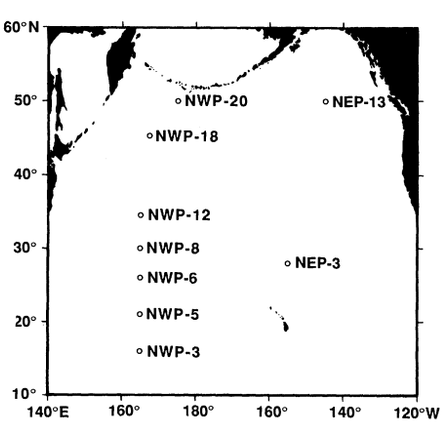

Fig. 1. Stations for the eastern and western North Pacific cruises on the R.V. *Discoverer* in June and July 1985 and May and June 1982, respectively.

Table 1. Concentrations of Sr and Sr/Cl ratios for selected stations in the eastern and western North Pacific. Uncertainties are given at the lσ level.

Depth (m)	Salinity (g/kg)	Sr (μg/kg)	Sr/Cl (μg/g)
	NEP-3, 2 July 1985		
	28°0.14'N, 154°58.4'W		
10	35.380	7672	392 ± 2
20	35.378	7682	392 ± 2
47	35.384	7372	392 ± 3
70	35.351	7633	390 ± 3
89	35.308	7760	397 ± 3
113	35.289	7741	396 ± 3
134	35.093	7713	397 ± 3
157	34.891	7636	395 ± 3
178	34.770	7646	397 ± 2
232	34.548	7667	401 ± 3
273	34.349	7619	401 ± 2
320	34.241	7532	397 ± 5
396	34.197	7552	399 ± 3
458	34.094	7591	402 ± 5
601	34.019	7572	402 ± 2
710	34.078	7552	400 ± 4
801	34.196	7688	406 ± 3
1010	34.391	7795	409 ± 3
1250	34.500	7736	405 ± 3
1493	34.554	7735	404 ± 4
2000	34.608	7735	404 ± 3
2508	34.642	7745	404 ± 3
2995	34.661	7744	404 ± 3
3505	34.675	7783	406 ± 5
3998	34.681	7783	405 ± 4
4508	34.686	7783	405 ± 3
4997	34.688	7783	405 ± 4
	NEP-13, 16 July 1985		
	49°58.3'N, 145°03.3'W		
2	32.568	7346	407 ± 3
10	32.577	7140	396 ± 2
25	32.572	7199	399 ± 3
50	32.624	7267	402 ± 4
75	32.635	7267	402 ± 3
100	32.656	7296	404 ± 2
125	33.088	7401	404 ± 2
150	33.665	7525	404 ± 3
175	33.752	7466	400 ± 4
199	33.784	7495	401 ± 4
225	33.809	7368	394 ± 3
255	33.839	7407	395 ± 4
299	33.881	7407	395 ± 2
349	33.952	7328	390 ± 3
400	33.817	7407	396 ± 3
501	34.098	7406	392 ± 3
598	34.180	7757	410 ± 3
701	34.245	7698	406 ± 3
799	34.288	7795	411 ± 4
899	34.326	7766	409 ± 3
1003	34.366	7766	408 ± 3
1250	34.441	7795	409 ± 1
1499	34.504	7755	406 ± 3
1750	34.558	7765	406 ± 4
1998	34.570	7764	406 ± 4
2499	34.626	7764	405 ± 5
2999	34.654	7764	405 ± 5
3496	34.670	7822	408 ± 2
4002	34.678	7822	408 ± 5
4240	34.679	7793	406 ± 4
	NWP-8, 7 June 1982		
	30°2.5'N, 165°07.0'E		
40	34.893	7743	401 ± 4
109	34.761	7646	397 ± 1
208	34.723	7646	398 ± 2
307	34.591	7618	398 ± 3
406	34.395	7678	403 ± 2
505	34.265	7590	400 ± 3
604	34.104	7464	395 ± 2
704	33.996	7543	401 ± 3
802	34.053	7494	398 ± 4
1000	34.238	7649	404 ± 2
1248	34.400	7717	405 ± 2
1496	34.494	7706	404 ± 3
1997	34.586	7706	403 ± 2
2161	34.610	7754	405 ± 4
2480	34.636	7754	404 ± 3
2964	34.660	7774	405 ± 1
	NWP-12, 10 June 1982		
	34°57.3'N, 164°58.7'E		
48	34.722	7715	401 ± 2
118	34.545	7745	405 ± 4
218	34.450	7814	410 ± 4
318	34.287	7747	408 ± 1
416	34.140	7816	414 ± 3
518	33.933	7748	412 ± 3
619	33.987	7651	407 ± 2
717	34.090	7562	401 ± 3
818	34.177	7620	405 ± 2
1017	34.295	7649	403 ± 3
1266	34.408	7785	409 ± 4
1516	34.493	7784	408 ± 3
2040	34.584	7755	405 ± 3
2210	34.604	7755	405 ± 2
2538	34.635	7754	404 ± 3
3032	34.657	7754	404 ± 3
3526	34.672	7754	404 ± 3
4012	34.679	7754	404 ± 2
4515	34.684	7754	404 ± 3
5017	34.683	7754	404 ± 2
	NWP-18, 17 June 1982		
	45°17.4'N, 167°15.0'E		
73	33.108	7108	388 ± 3
143	33.403	7263	393 ± 5
243	33.698	7242	388 ± 6
344	33.968	7367	392 ± 7
443	34.000	7318	389 ± 7
542	34.149	7396	391 ± 4
642	34.229	7444	393 ± 4
742	34.274	7395	390 ± 6
842	34.322	7414	390 ± 4
1040	34.410	7443	391 ± 6
1291	34.476	7492	393 ± 3
1540	34.535	7569	396 ± 4
2040	34.613	7676	401 ± 7
2209	34.617	7676	401 ± 4
2538	34.639	7725	403 ± 4
3038	34.664	7783	406 ± 4
	Copenhagen water, P-90		
	35.003	7742	400 ± 1

seas, which show acantharians as a major component of surface marine plankters, often exceeding the numbers of their protozoan counterparts, radiolarians and foraminifera (*2, 5–8, 22*).

In our study, acantharian skeleton and cyst fluxes were derived from free-drifting sediment traps deployed along latitudinal transects in both the eastern and western North Pacific Ocean. Particulate fluxes were compared to Sr/Cl profiles and model calculations for the fluxes of dissolved Sr. These results show the important role of acantharians in the ocean's Sr budget.

Samples for this study were collected in the western North Pacific Ocean in May and June 1982 and in the eastern North Pacific Ocean in June and July 1985 during cruises aboard the *Discoverer*, a research vessel of the National Oceanic and Atmospheric Administration. Seven stations were located in the northwest Pacific Ocean (NWP-3 through NWP-20) along a transect between 16° and 50°N, and two stations (NEP-3 and NEP-13) were located in the northeast Pacific Ocean at 28° and 50°N (Fig. 1).

Free-floating, modified (*23*) Soutar-type sediment traps (*24*) were used to funnel settling particulates into a Teflon collection cup located at the base of each trap. Traps were deployed individually. To ensure sample isolation at discrete depths and to provide known collection times (on the order of 25 hours), a double-seal, ball-valve system was activated by a preset electronic release before trap retrieval.

In the northwest Pacific Ocean, sediment traps were deployed between 100- and 2170-m water depths. Sediment trap samples from the northeast Pacific Ocean were obtained from water depths ranging from 100 to 3500 m. When possible, replicate samples were obtained.

When the traps were retrieved, sample particulates were immediately filtered onto acid-washed Nuclepore filters (47 mm in diameter, 0.4-μm pore size) and rinsed briefly with distilled-deionized water to prevent the formation of salt crystals. Samples were stored in a vacuum desiccator over silica gel until they could be transferred to a shore-based, clean facility for analysis.

To minimize sample contamination, all work was conducted either in a clean room, where the temperature and relative humidity were maintained at 20°C and 40%, respectively, or within a vertical-flow clean bench. Acantharian skeletons and cysts were identified under a reflected light stereomicroscope (magnification, ×80). The organisms were mechanically transferred to 47- or 25-mm preweighed filters by using either triple-0 or Japanese calligraphy brushes dipped in distilled-deionized water. After desiccation under vacuum and over silica gel, these isolated acantharian specimens were weighed on a Perkin-Elmer autobalance. Acantharian $SrSO_4$ fluxes (in micrograms per square meter per day) were subsequently calculated from the weights. An ISI-DS-130 scanning electron microscope was used to obtain photomicrographs of various acantharian skeletons and their cysts. An energy-dispersive x-ray analyzer (EDXA) system (Kevex 7000) was used to confirm the $SrSO_4$ composition of both skeletons and cysts.

Dissolved Sr samples were drawn from 30-liter Niskin bottles into acid-cleaned, 125-ml amber polyethylene bottles for later laboratory analysis. These samples were obtained at stations NWP-8, NWP-12, and NWP-18 and at stations NEP-3 and NEP-13.

Strontium samples were analyzed by using a Perkin-Elmer 603 atomic absorption spectrophotometer with a PRS10 printer sequencer in parallel with a strip chart recorder. To prevent salt buildup on the nebulizer, samples were diluted by a factor of 5. Standards, in concentrations ranging from 0.5 to 2.5 mg of Sr per liter, were prepared by appropriate dilutions of Titrisol atomic absorption standard $SrCl_2$. The sodium content of the standards was matched to that of the samples by composing the standards in a

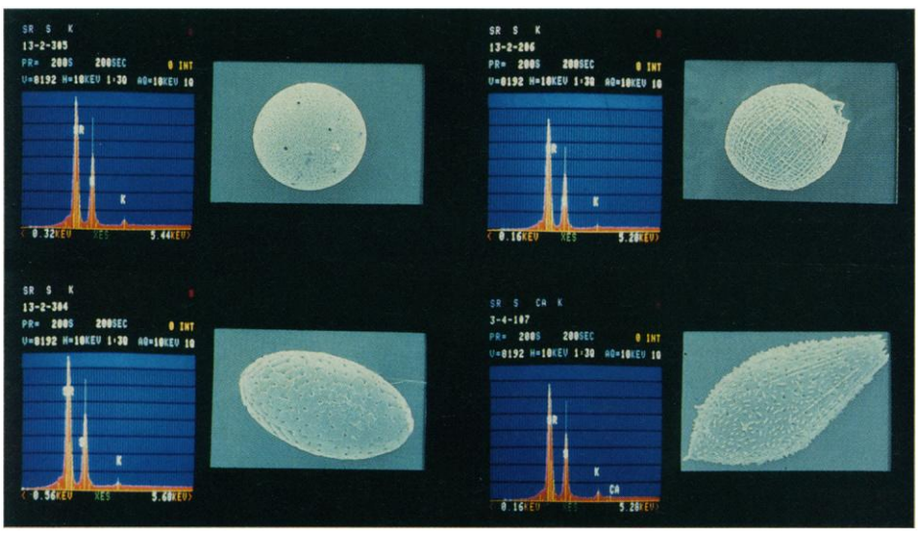

Fig. 2. Four acantharian specimens with their corresponding EDXA spectra showing their $SrSO_4$ composition. Specimen dimensions follow. Lower right: 190 μm long and 100 μm wide; lower left: 118 μm long and 55 μm wide; upper right: 80 μm in diameter; upper left: 165 μm in diameter.

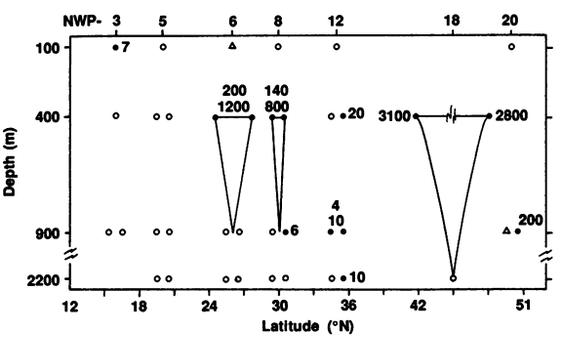

Fig. 3 (left). Acantharian $SrSO_4$ fluxes derived from western North Pacific sediment trap deployments. Closed circles represent a measured flux. Numbers associated with closed circles depict fluxes in micrograms per square meter per day. Open circles represent nondetectable fluxes. Open triangles indicate a sediment trap deployment with acantharian specimens too few or too small to be weighed. Horizontal lines provide a graphic depiction of the average flux at each depth. **Fig. 4 (right).** Acantharian $SrSO_4$ fluxes derived from eastern North Pacific sediment trap deployments. Symbols are the same as those in Fig. 3.

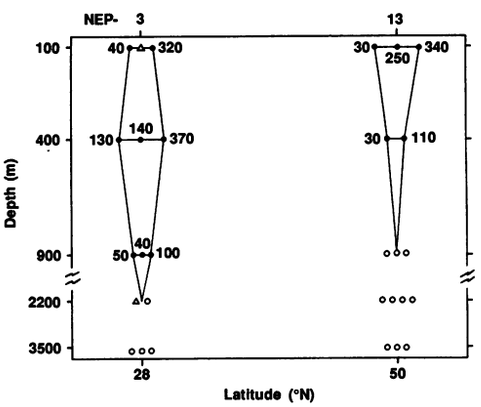

0.5*M* solution of NaCl. To monitor instrumental drift during the course of these analyses, a secondary standard of Copenhagen water was also prepared (P-90, Cl = 19.3755 per mil). Lanthanum was added to both the standards and the samples to prevent interference (final concentration of 10 g of lanthanum per liter) from Si, Al, phosphate, and sulfate. During analyses, an initial standard curve was run and samples were subsequently interspersed with blanks. Blanks averaged 0.08 ± 0.03 (1σ) mg of Sr per liter. Samples were run in quadruplicate and yielded 1σ standard deviations ranging from ±0.34 to ±1.8%. Results of samples analyzed by atomic absorption spectroscopy were then compared with those obtained by using inductively coupled plasma emission spectrometry. The two techniques provided similar results. Salinities were analyzed at sea with a Guildline autosal salinometer.

After EDXA confirmation of acantharian skeleton and cyst composition (Fig. 2), our gravimetrically derived acantharian fluxes were translated into $SrSO_4$ fluxes. Vertical $SrSO_4$ fluxes below 100 m show similar patterns on both sides of the ocean (Figs. 3 and 4). The 100-m fluxes in the western Pacific are low to nondetectable, whereas those in the eastern Pacific are comparable to the 400-m flux values from the same stations. On both sides of the North Pacific, maximum fluxes are generally observed at 400 m. By 900 m most acantharian $SrSO_4$ seems to be mobilized, and in only one case (NWP-12) was a flux detectable at 2170 m. No acantharian specimens were found in the 3500-m traps. The sharp decrease in flux values between 400 and 900 m indicates a rapid mobilization of acantharian-derived $SrSO_4$, which appears complete by 3500 m.

Nonuniform acantharian distribution is indicated by variable replicate sample flux values. This is consistent with previous biological work on standing crops of these organisms (*3, 25*).

Data on dissolved Sr from the stations located on both sides of the North Pacific are given in Table 1. The Sr/Cl profiles are depicted in Fig. 5. In the upper kilometer of the water column, Sr/Cl ratios are not constant with depth. The largest Sr/Cl variation, 390 to 411 μg/g, was observed at NEP-13, and the smallest variation, 395 to 405 μg/g, was observed at NWP-8. Low Sr/Cl ratios generally occur within the upper 700 m of the water column. Below these depths there is often an intermediate maximum between 700 and 1250 m. From there to the abyssal depths, Sr concentrations and Sr/Cl ratios tend to stabilize.

To our knowledge, these sediment trap collections are the first to exhibit acantharian specimens. Relatively shallow sampling depths along with short-term deployment times permitted the collection of these labile marine components.

Whether the synthesis and subsequent dissolution of acantharian skeletons and cysts have a perceptible impact on the dissolved Sr in the water column might be ascertained by correlating $SrSO_4$ flux values with variations in Sr/Cl ratios. Although Sr/Cl ratios reflect the long-term integration of processes influencing Sr, and flux data derived from short-term deployment of sediment traps provide essentially a "snapshot" view, comparison of the two data sets points to certain immediate observations and correlations. Both data sets indicate an uptake of Sr in the upper waters and a release at intermediate depths. This is followed, at greater depths, by a stabilization in the processes affecting dissolved Sr. Uptake of Sr in the upper waters is consistent with data by Bishop *et al.* (*8, 9*) and Michaels (*11*), which show acantharian standing stocks to have a near-surface maximum. Subsequent mobilization of Sr at intermediate depths appears to be nearly complete by 1000 m. Comparison of averaged 400-m fluxes (224 μg m^{-2} day^{-1}) to an average of corresponding 900-m fluxes (13 μg m^{-2} day^{-1}) indicates a 94% flux diminution between these horizons. At greater depths, only one out of seven stations (NWP-12, 2170 m) produced a detectable flux. This rapid attenuation of acantharian $SrSO_4$ fluxes precludes further influence on dissolved Sr, thereby accounting for the relatively constant Sr/Cl ratios below 1250 m.

Although a depth-by-depth correlation between flux data and Sr/Cl ratios is not assured because of the different integration times inherent in the data sets, one such correlation is particularly striking. From among all our stations, the lowest Sr/Cl ratios are evident in shallow waters at station NWP-18, which is located in the highly productive waters of the subpolar gyre. This shallow Sr/Cl minimum is correlated with the highest flux value (NWP-18, 400 m) in our data set. High fluxes, possibly indicative of a large Sr uptake, may well account for

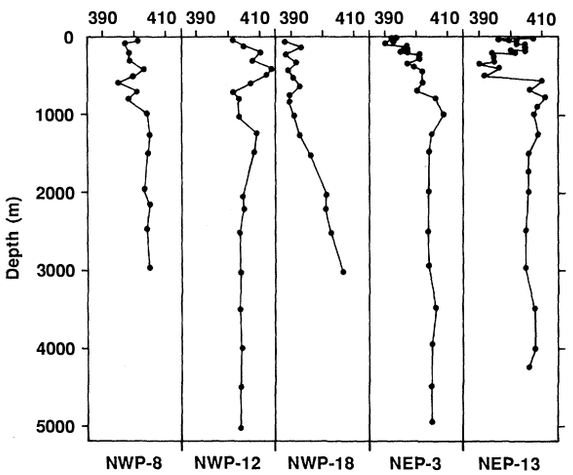

Fig. 5. Profiles of Sr/Cl for selected stations in the eastern and western North Pacific (Sr in micrograms per kilogram; Cl in grams per kilogram; Sr/Cl in micrograms per gram).

Table 2. Model parameters and estimates of in situ strontium dissolution in the North Pacific. Uncertainties are given at the 1σ level. Abbreviations: J/W, dissolution flux/upwelling velocity; W/K_z, upwelling velocity/vertical eddy diffusion coefficient.

Station	Date	Latitude	Longitude	W/K_z (km^{-1})	J/W (mg kg^{-1} km^{-1})	Integrated flux (g m^{-2} $year^{-1}$)	Sediment trap flux (g m^{-2} $year^{-1}$)
NWP-6	4 June 1982	26°11.2′N	165°11.5′E	−1.53			0.44
NWP-8	7 June 1982	30°02.5′N	165°07.0′E	−1.97	0.23	0.50 ± 0.25	0.29
NWP-12	10 June 1982	34°57.3′N	164°58.7′E	−1.40	0.14	0.31 ± 0.15	
NWP-18	17 June 1982	45°17.4′N	167°15.9′E	−1.26			1.13
NEP-3	2 July 1985	28°01.4′N	154°58.4′W	−2.93	0.49	0.67 ± 0.33	0.08
NEP-13	16 July 1985	49°58.3′N	148°03.3′W				0.08

low corresponding shallow water Sr/Cl ratios.

Our observations of considerable $SrSO_4$ fluxes at 400 m are supported by Brass's (*14*) multiple flux estimates for surface Pacific waters. Based on three independent sets of parameters, Brass's (*14*) estimates range from 1264 to 2297 μg of $SrSO_4$ per square meter per day, even larger than the average of all our 400-m fluxes (565 μg m^{-2} day^{-1}). In apparent contrast to our observations, the measurements of Bishop *et al.* (*8*) from the Atlantic suggest that most acantharian skeletons are mobilized above 400 m. Thus, the acantharian specimens in our trap samples may represent only a fraction of the total number originally descending through the water column.

Our flux observations may be attributable to a robust particulate fraction that does not undergo extremely shallow mobilization. Bishop *et al.* (*8*) reported that a typical acantharian skeleton contains approximately 0.2 nmol of Sr. Shallow sediment trap observations of acantharians settling out of the euphotic zone (*26*) reveal "typical" forms having 20 relatively thin celestite spines. In contrast, acantharians in our samples contained from 5 to 49 nmol of Sr (based on mean weights of groups of acantharians) and consisted primarily of comparatively robust cysts and a few of the more heavily skeletalized acantharian species. Surface-to-volume ratios suggest that these robust specimens may dissolve more slowly than typical acantharian skeletons. Consequently, we can resolve two overlapping patterns of particulate Sr flux: (i) a shallow, rapid regenerative cycle in the upper 200 m that involves large numbers of typical acantharians, which contain little Sr and dissolve rapidly and (ii) a deeper, slower regenerative cycle that involves the movement of relatively few, heavily skeletalized forms (predominately acantharian cysts) into intermediate waters where dissolution ultimately occurs. According to this hypothesis, it is the robust acantharian specimens that account for high 400-m fluxes and the intermediate Sr/Cl maximum between 700 and 1250 m.

In an independent assessment of the Sr fluxes, a one-dimensional diffusion-advection model was used for our data set on dissolved Sr. This model, previously used for oxygen (*27*) and total carbon (*28*), depicts, in our case, vertical dissolution profiles between the minimum and maximum Sr/Cl ratios for each station. Our model was limited to depth intervals over which the temperature-salinity relation was linear. Scale height, which is the ratio W/K_z, at each station was determined from either salinity or potential temperature data (W is upwelling velocity and K_z is the vertical eddy diffusion coefficient). The upwelling velocity was assumed to be 4.5 m $year^{-1}$, which is the mean of the most recent estimates for the North Pacific (*28, 29*). Table 2 presents a comparison of modeled vertical fluxes for Sr and corresponding dissolution fluxes estimated from the sediment traps.

In the two cases where a direct comparison of the two techniques can be made, the estimate from the traps is lower than that derived from the model. This is consistent with the model's neglect of potentially significant horizontal flux effects as well as the potential problem of acantharian $SrSO_4$ underestimations due to dissolution or fragmentation during the course of sediment trap sampling and specimen manipulation. Within the context of such uncertainties and the inherent difficulties encountered in comparisons that cannot account for temporal variations, flux estimates that are derived from sediment traps are in surprising agreement with those modeled from data on dissolved Sr.

The emergent picture is one of acantharian-mediated Sr/Cl trends in upper and intermediate waters. However, new evidence suggests that hydrographic conditions may also play a role in the delineation of Sr/Cl profiles. Stable lead isotope data from the eastern Pacific (*30*) indicate that horizontal advection strongly influences the composition of the upper kilometer of the water column. Although the extent to which our profiles are influenced by advective forces remains unresolved, horizontal advection effects might account for some of the fine-scale Sr/Cl perturbations observed in our profiles.

Maximum surface acantharian standing stocks are inconsistent with our low 100-m fluxes in the northwest Pacific. Highly variable horizontal and vertical acantharian distributions as well as grazing by swimmers provide possible explanations. In addition, the labile nature of a majority of the surface-dwelling acantharians points to their potentially rapid dissolution in shallow traps. Consequently, decreases in our processing times of shallow traps between the western and eastern Pacific stations may also contribute, in part, to the flux differences that we observed at shallow depths.

Despite the dearth of information on acantharian bioecology, it seems clear from our study that these marine organisms have a perceptible influence on the ocean's strontium budget. As a further consequence of their surface water abundance and the subsequent dissolution of significant amounts of acantharian-synthesized $SrSO_4$ in intermediate waters, acantharian specimens may also constitute an important vector for trace metal transport (*13–15*).

REFERENCES AND NOTES

1. A. Hollande and M. Enjumet, *C. R. Acad. Sci.* **244**, 508 (1957); A. Hollande, J. Cachon, M. Cachon-Enjumet, *Protistologica* **1**, 91 (1965); E. M. Bottazzi, *Ist. Lomb. Accad. Sci. Lett. Rend. Sci. Biol. Med. B* **107**, 3 (1973).
2. E. M. Bottazzi, *Boll. Zool.* **45**, 133 (1978).
3. ——— and M. G. Andreoli, *J. Plank. Res.* **4**, 757 (1982).
4. J. R. Beers and G. L. Stewart, *Limnol. Oceanogr.* **15**, 825 (1970).
5. E. M. Bottazzi, B. Schreiber, V. T. Bowen, *ibid.* **16**, 677 (1971).
6. J. R. Beers and G. L. Stewart, *Deep Sea Res.* **18**, 861 (1971).
7. J. R. Beers, F. M. H. Reid, G. L. Stewart, *Int. Rev. Gesamten Hydrobiol.* **60**, 607 (1975).
8. J. K. B. Bishop, J. M. Edmond, D. R. Ketten, M. P. Bacon, W. B. Silker, *Deep Sea Res.* **24**, 511 (1977).
9. J. K. B. Bishop *et al.*, *ibid.* **25**, 1121 (1978).
10. L. B. Graham, A. D. Colburn, J. C. Burke, *Limnol. Oceanogr.* **21**, 336 (1976).
11. A. F. Michaels, in preparation.
12. G. W. Brass and K. K. Turekian, *Earth Planet. Sci. Lett.* **23**, 141 (1974).
13. G. Arrhenius, in *The Earth Beneath the Sea*, vol. 3 of *The Sea*, M. N. Hill, Ed. (Interscience, New York, 1963), p. 678; N. Rieder, H. A. Ott, P. Pfundstein, R. Schoch, *J. Protozool.* **29**, 15 (1982); R. Collier and J. Edmond, *Prog. Oceanogr.* **13**, 113 (1984).
14. G. W. Brass, *Limnol. Oceanogr.* **25**, 146 (1980).
15. The reported elemental composition of acantharia (*13, 14*) includes a wide variety of metals (for example, Ba, Cu, Zn, Pb, Fe, and Rb). Barium is a particularly notable constituent, with a Ba/Sr ratio near 4×10^{-3}.
16. M. A. Desgrez and J. Meunier, *C. R. Acad. Sci.* **183**, 689 (1926).
17. H. T. Odum, *Science* **114**, 211 (1951).
18. T. J. Chow and T. G. Thompson, *Anal. Chem.* **27**, 18 (1955).
19. F. T. Mackenzie, *Science* **146**, 517 (1964); R. Culkin and R. A. Cox, *Deep Sea Res.* **13**, 789 (1966); B. P. Fabricand, E. S. Imbimbo, M. E. Brey, J. A. Weston, *J. Geophys. Res.* **71**, 3917 (1966).
20. M. Bernat, T. Church, C. J. Allegre, *Earth Planet. Sci. Lett.* **16**, 75 (1972).
21. G. W. Brass and K. K. Turekian, *ibid.*, p. 117.
22. E. M. Bottazzi and M. G. Andreoli, *Ateneo Parmense Acta Nat.* **14**, 465 (1978); *ibid.*, p. 477.
23. P. R. Betzer *et al.*, *Deep Sea Res.* **31**, 1 (1984); P. R. Betzer *et al.*, *Science* **226**, 1074 (1984).
24. A. Soutar, S. A. Kling, P. A. Crill, E. Duffrin, K. W. Bruland, *Nature (London)* **266**, 136 (1977).
25. E. M. Bottazzi and M. G. Andreoli, *Arch. Oceanogr. Limnol.* **18**, 115 (1974).
26. A. F. Michaels, unpublished data.
27. K. Wyrtki, *Deep Sea Res.* **9**, 11 (1962).
28. H. Craig, *J. Geophys. Res.* **74**, 5491 (1969).
29. S. Tsunogai, *J. Oceanogr. Soc. Jpn.* **28**, 145 (1972); B. J. Peterson, *Ocean Sci. Eng.* **6**, 71 (1981); W. S. Broecker and T. H. Peng, *Tracers in the Sea* (Lamont-Doherty Geological Observatory, Palisades, NY, 1982).
30. A. R. Flegal, K. Itoh, C. C. Patterson, C. S. Wong, *Nature (London)* **321**, 689 (1986); A. R. Flegal, personal communication.

31. We thank Captains R. Speer and S. Peterson and the crews of the R.V. *Discoverer* for helping to make the respective 1982 and 1985 cruises productive. The deck crews under the supervision of A. Kirsch and W. Sherril were indispensable. We thank K. Roe for support with the Sr analyses. T. Irving provided the inductively coupled plasma analyses and K. Takahashi guided us in establishing the presence of cysts in the samples. We thank T. Greco for darkroom work as well as EDX analyses. Supported in part by grants from NSF (OCE 85-00739) and the Department of Energy (19X-27404C). Contribution No. 904 from the Pacific Marine Environmental Laboratory.

14 January 1987; accepted 6 July 1987